Journal of Photochemistry & Photobiology, B: Biology 182 (2018) 122–129

Contents lists available at ScienceDirect

Journal of Photochemistry & Photobiology, B: Biology

journal homepage: www.elsevier.com/locate/jphotobiol

Chemically synthesized butein and butin: Optical, structure and electrochemical redox functionality at electrode interface

Priya Darshani[a], Manju Bhargavi Gumpu[b,c], Prasanth Thumpati[a], John Bosco Balaguru Rayappan[b,c], Velayutham Ravichandiran[a], Gururaja Perumal Pazhani[a,*], Murugan Veerapandian[d,*]

[a] National Institute of Pharmaceutical Education and Research, Kolkata 700032, West Bengal, India
[b] Nano Sensors Lab @ Centre for Nanotechnology & Advanced Biomaterials (CeNTAB), SASTRA University, Thanjavur 613 401, Tamil Nadu, India
[c] School of Electrical & Electronics Engineering, SASTRA University, Thanjavur 613 401, Tamil Nadu, India
[d] Electrodics and Electrocatalysis Division, CSIR-Central Electrochemical Research Institute, Karaikudi 630 003, Tamil Nadu, India

ARTICLE INFO

Keywords:
Chalcone
Flavanone
Photoluminescence
Electrochemical fingerprinting
Redox behavior

ABSTRACT

Progress in the development of phytochemistry has delivered advancement in materials functionality for range of inter/trans-disciplinary application. Here, we investigated the structural functionality of chemically synthesized phytoconstitutent, chalcone (butein) and flavanone (butin). Photoactive and electroactive behavior of butein and butin were comprehensively studied using UV–vis absorbance, photoluminescence and cyclic voltammetric techniques. Surface morphology of the butein and butin powders was characterized from scanning electron microscope at an operating voltage of 10 kV. Significant ultraviolet absorbance property are observed from butein and butin due to the distribution of $\pi \rightarrow \pi^*$ and $n \rightarrow \pi^*$ transitions. Photoluminescence emission spectra of the prepared materials are well resolved at visible region *via* keto-enol tautomerization and can be influenced by solvent pH. Cyclic voltammetric studies on the prepared materials enabled a direct electron-transfer reaction at gold-screen printed electrode, indicating the feasibility for analytical validation in herbal industries. Existence of multiple electroactive hydroxyl groups makes butein and butin a redox-functional species at electrode interface. Dispersion ability in aqueous and organic solvents makes butein and butin suitable for variety of photochemical applications. This phytochemical material offers new degrees of optical and redox functionality similar to inorganic nanostructures, in addition to inherent bioactivity, that may be advantageous for further biomedical function.

1. Introduction

Bio-friendly optical and electrochemical active materials are advantageous for interdisciplinary application in biosensor, molecular probe and drug delivery system [1,2]. Phytochemicals are recently emerging as potential candidate for development of biomedical functional materials [3]. Secondary metabolites of plant particularly flavonoids have significant biochemical and physiological functionality, *viz.*, radical scavenging, anti-inflammatory, anti-mutagenic and anti-microbial to name a few [4,5]. Spectroscopic studies on flavonoids revealed the distinct fluorescence emission property [6], perhaps similar to plasmonic nanostructures which are interesting for molecular probe development. Further, natural pigment molecules having porphyrin/pthalocyanine-like structures are explored in photonic and electrochemical applications, with or without combination of nanostructures [7–11]. Therefore, scalable synthesis of biologically important phytochemicals and exploring the novel physico-chemical properties are useful for translational studies. Chemical structures of flavonoids are featured by a 15-carbon backbone (C6—C3—C6) comprising of two benzene rings A and B linked with a heterocyclic pyrane ring C (Fig. 1) [12,13]. Major subclasses of flavonoid structures are chalcones, flavanones, flavanols, flavones, isoflavones and anthocyanins. Butein ((E)-1-(2′,4′-dihydroxyphenyl)-3-(3,4-dihydroxyphenyl) prop-2-en-1-one), is a chalcone type flavonoids with a potential anti-oxidant property. Butein is a vital dietary polyphenol have the capability to inhibit protein tyrosin kinase, thus preventing phosphorylation and affording inflammatory modulating effect and anti-cancer activity [13]. This was well explored in various clinical conditions like colon carcinoma [14], myelogenous leukemia [15], breast carcinoma [16], hepatic carcinoma [17] and restenosis (narrowing of blood vessel) [18]. Butein is often

* Corresponding authors.
E-mail addresses: pazhanigp@gmail.com (G.P. Pazhani), vmurugan@cecri.res.in (M. Veerapandian).

https://doi.org/10.1016/j.jphotobiol.2018.04.001
Received 18 February 2018; Received in revised form 20 March 2018; Accepted 2 April 2018
Available online 06 April 2018
1011-1344/

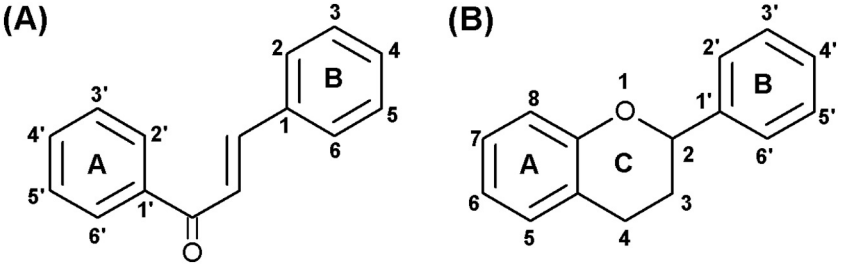

Fig. 1. Fundamental structure of (A) chalcone and (B) flavanone.

isolated from the genera *Dahlia*, *Butea*, *Searsia* and *Coreopsis*. Owing to its extensive pharmacological properties nowadays butein is chemically synthesized, for bulk herbal formulation, using base-catalyzed aldol/Claisen-Schmidt condensation or acid-mediated aldolization of o-hydroxyacetophenone and benzaldehyde. Likewise, butin is a bioactive flavanone cyclized form of butein and chemically 2-(3,4-dihydroxyphenyl)-7-hydroxychroman-4-one. Park et al., studied that the major bio-constituent of *Rhus verniciflua* Stokes extracts *i.e.,* butin inhibited the CYP19-mediated estrone formation in a concentration dependent manner and having modulatory effect on androgen hormone levels, which may lead to a molecule for aromatase inhibitors [19].

Biological merits of butein/butin can be tuned by their pharmacological dosage which indeed governed by the analytical validation. Thus, sensitive quantification of butein/butin is beneficial for ensuring the dosage in polyherbal formulation. High-performance liquid chromatography (HPLC) is the conventional method in practice for testing the flavonoids/polyphenols from plant extracts and often coupled with UV or fluorescent detectors for the separation and characterization. Recently, HPLC integrated mass spectrometry equipped with atmospheric pressure chemical ionization (APCI) or electrospray ionization are explored for the identification and quantification of several phenolic compounds from natural products [20]. Although these techniques are advanced and provide sensitive quantification of active phytochemicals, still there are limitations associated with these methods like need of sophisticated instrumentation, labor-intensive/time consuming operation and expensive in assay cost. Thus, modern pharmaceutical/nutraceutical industries demands user-friendly, rapid and reliable method for quantification of phytochemicals without complex sample pre-treatment.

Electrochemical sensors are recently emerging as an important analytical tool for rapid, sensitive and cost-efficient testing of various analytes *viz.,* biomolecule/biomarkers of clinical value [21–23], environmental pollutants [24,25] and intermediate chemicals [26]. Due to its integration feasibility with modern gadgets, simple instrumentation and user-friendliness, electrochemical sensors are optimal for portable device fabrication and on-site utility. Significant electrochemical sensing reports on active flavonoids are available in the literature. For instance, mangiferin is a flavonoid with glycosylated structure (2-β-D-glucopyranosyl-1,3,6,7-tetrahydroxy-9H-xanthen-9-one) commonly found in fruits, leaves, stem bark and root of *Mangifera indica* [27]. Tajik et al. [28], have demonstrated a carbon paste electrode modified with graphene nanosheets and an ionic liquid (*n*-hexyl-3-methylimidazolium hexafluoro phosphate) for the electrochemical study of mangiferin. Sims et al. [29], have used multi-walled carbon nanotubes-modified basal-plane pyrolytic graphite electrode as sensor platform for the detection of hesperidin. Wang et al. [30], have hydrothermally synthesized the CeO_2-poly(diallyldimethyl ammonium chloride)-graphene based nanocomposite and demonstrated their electrochemical sensing of eriocitrin (eriodictyol 7-O-β-rutinoside), a flavanone glycoside abundant in lemon/lime. Xie et al., [31] have reported an integrated electrochemical sensor, based on bimetallic oxide particles composite, *i.e.,* tantalum oxide (Ta_2O_5), niobium oxide (Nb_2O_5) and chitosan (CTS) modified carbon paste electrode (Ta_2O_5-Nb_2O_5@CTS-CPE) for individual and simultaneous detection of baicalein (a flavonoid glucuronides) and baicalin (a glycone baicalein). Both are main bioactive constituents of Chinese medicinal herb, *Scutellariae radiax*. To the best of authors' knowledge, only couple of electrochemical studies on butein is available in the literature. For instance, Hodnick et al. [32], explored the voltammetric behavior of butein at glassy carbon electrode (GCE) using 0.1 M phosphate buffered solution (PBS) of pH 7.5 constituting a final concentration of 2.5% (v/v) of dimethyl sulfoxide. Tesio et al. [33], has evaluated the electrochemical oxidation of butein at GCE using phosphate and citrate solutions of different pH values and 1 M perchloric acid-aqueous solution using voltammetric techniques. In this study, we report the chemical synthesis of butein/butin and study the optical, chemical structure and distinct redox behavior at electrode interface, with respect to scan rate and pH. Fundamental possibility on direct electrochemical probing of butein and butin were also performed, distinctly using unconventional screen printed electrode, straightforward for real-time application at the industrial site. Compared to conventional disintegrated three electrode system, single chip based screen-printed electrodes on flexible matrix are advantageous allowing cost-efficient assay of target with minimal sample volume.

2. Experimental Section

2.1. Materials and Methods

2,4-dihydroxyacetophenone and 3,4-dihydroxybenzaldehyde were purchased from Spectrachem Pvt., Ltd. Silica gel (100–200 mesh size), potassium hydroxide (KOH) and sodium hydroxide (NaOH) pellets were procured from Sisco Research Laboratories Pvt., Ltd., India. TLC plates were from Merck. Other chemicals and solvents (ethanol (EtOH) and methanol (MeOH)) were of analytical standard and used as received without further purification. Deionized water from a Millipore system with resistivity > 18.2 MΩ/cm was used for all experimental solutions.

Optical absorbance of the synthesized butein and butin was studied from Jasco V-550 spectrophotometer. Chemical structure and functional group modifications on the butein and its cyclized form (butin) were characterized using Fourier transform infrared (FTIR) spectroscopy using JASCO FT-IR 4200. Scanning electron microscopic images were studied from TESCAN, model: VEGA3 with an acceleration voltage of 10 kV. ^{1}H NMR spectral studies were obtained from Bruker Avance III 600 MHz. Electrochemical analyses were performed using a hand-held potentiostat (PalmSens3, Netherlands). Photoluminescence (PL) spectral analysis was studied from spectrofluorometer (Varian, Cary Eclipse). Cyclic voltammogram and sensing studies were tested using screen printed electrodes (SPE), (Model: AC1·W1.R1) from BVT Technologies, Czech Republic, comprised of an Au working electrode (geometric working area of 0.79 mm^2), Au counter electrode and Ag/AgCl as reference electrode.

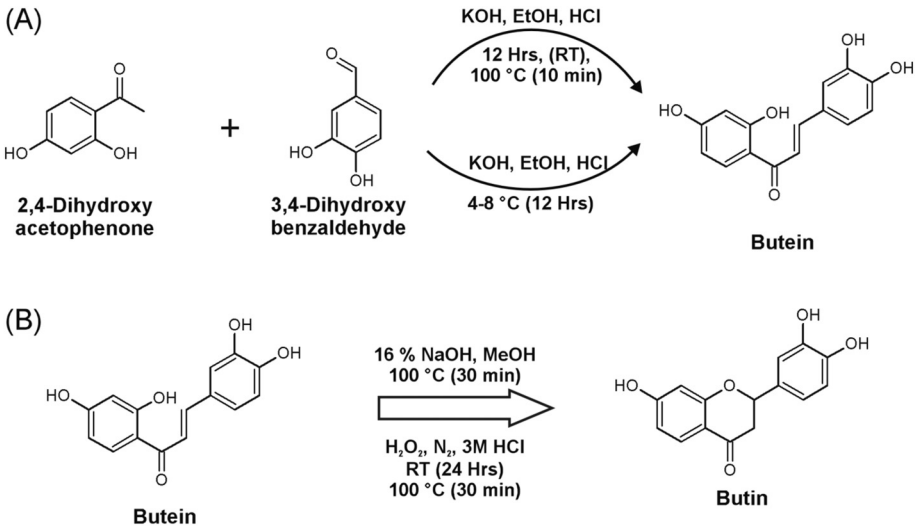

Scheme 1. Synthesis of (A) butein and (B) butin.

2.2. Synthesis and Purification of Butein

35 ml of aqueous KOH solution (50 g; 891 mM) was slowly added to a vial containing mixture of 2,4-dihydroxyacetophenone (5.5 g, 36 mM) and 3,4-dihydroxybenzaldehyde (5 g, 362 mM) in 15 mL ethanol. The resulting red colored mixture was heated at 100 °C for 30 min, under magnetically controlled stirring. Afterward the reaction mixture was incubated at ambient room temperature for 12 h. Then the mixture was diluted with equal amount of water and acidified with diluted HCl till the occurrence of yellow colored precipitate. Resulted product were filtered and dried with an aid of Buckner funnel under vacuum. Final purified product was obtained after column chromatography. Above reactions were also performed at cold conditions (4–8 °C) instead of 100 °C for 12 h, both conditions enabled an experimental yield of 60%. Briefly, the precipitates were solubilized in MeOH and mixed with silica gel to make slurry for the column and then dried under rotary evaporator. The column was wet packed using silica gel, 100–200 mesh size and solvent petroleum ether. Upon setting of bed slurry, the compound was added to the packed column. Fractions were collected by changing the concentration of solvent. Elution of desired compound was monitored by TLC with solvent petroleum ether and ethyl acetate (50:50%). Eluted fractions were evaporated in rotary evaporator, confirmed from TLC and then utilized for further characterization.

2.3. Synthesis of Butin

Under nitrogen environment, aqueous solution of 1.6 mL NaOH (16%) was slowly injected into a reaction vessel containing methanolic solution of butein (300 mg (1 mM) in 10 mL of MeOH) under stirring and then the reaction vessel was refluxed at 100 °C for 30 min. Afterward, 15% of H_2O_2 solution was added into the reaction vessel. Resulted mixture was incubated at room temperature for 24 h. After incubation, reacted content was diluted with 50 mL of ice cold water and acidified with 3 M HCl. Resulting precipitate was washed thrice with chloroform and then concentrated using rotary evaporator. As-obtained product was then air dried and purified using column chromatography, as described above.

3. Results and Discussion

Biosynthetic pathway for butein in plants such as *Aspergillus alliaceus* and *Dahlia variabilis* has been well elucidated [34,35]. For instance, in *A. alliaceus* trihydroxychalcone is converted to butein involving an enzymatic hydroxylation by cytochrome *p*450 and catechol oxidase. In the case of *D. variabilis,* three molecules of malonyl-CoA and a *p*-coumaroyl-CoA reacts to form trihydroxychalcone, in presence of chalcone synthase/chalcone reductase. Enzyme chalcone-3-hydroxylase converts the trihydroxychalcone to butein. Owing to its multiple health benefits, butein is widely synthesized by chemical method for large scale utility using Claisen-Schmidt aldol condensation. In this approach, the hydroxyl moieties of 2,4-dihydroxyacetophenone and 3,4-dihydroxybenzaldehyde were protected with allyl bromide, in presence of K_2CO_3 in DMF, and condensation was done in presence of KOH and MeOH. Alkyl-protecting groups were removed using microwave irradiation in presence of $PdCl_2(PPh_3)_2$ and ammonium formate to obtain butein [36]. Herein a simplified procedure was implemented using two different experimental conditions as illustrated in Scheme 1. Compared to ambient room temperature condition (yield 40%), the reaction undergone at cold condition (4–8 °C) exhibited a better yield (60%).

Similar to butein, biosynthetic pathway for butin also exist in the plants involving chalcone isomerase enzyme for conversion of chalcones into flavanone. General method for the synthesis of flavanone is cyclization of duly substituted 2-hydroxychalcone under distinct condition using acids and bases. Alternative approach for the synthesis of flavanone (*i.e.,* butin) include the oxidation of flavan-4-ol and the intermolecular oxa-Michael addition of activated α,β-unsaturated ketones [37]. Herein, the cyclization reaction chemistry of butein under nitrogen environment was supported by base catalysis in presence of H_2O_2 and acidification by HCl (Scheme 1B). Fig. 2(A) shows the UV–vis absorbance spectrum of methanolic solution of butein and butin. As can be seen butein has three significant absorption bands located in the UV region centered at 209 nm, 261 nm and 378 nm, which are ascribed to the $\pi \rightarrow \pi^*$ and n-π^* transition, respectively. An additional shoulder hump centered at 307 nm is attributed to the intramolecular charge transfer. Likewise, butin exhibited three absorption bands at 208, 257 and 382 nm. Observed minor shift in the bands of butin sample with a disappearance of shoulder hump at 307 nm indicates the existence of cyclized form of butein. The full width at half maximum (FWHM) for the absorbance peak at 382 nm for butin sample is found to be 67.15 nm, while FWHM for butein at 378 nm is 59.22 nm. Fig. 2(B) shows the intact morphological features of butein and butin powder samples prepared on the carbon tape. As-synthesized/purified butein and butin samples exhibit the microstructural clusters. Compared to butein, butin samples are in disintegrated form with a topography of crystal-like structures. Both samples were visualized at an operating acceleration voltage of 10 kV. Further analysis on the functional groups of butein/butin and its associated vibrational information are evaluated from FT-IR spectral analysis (Fig. 3).

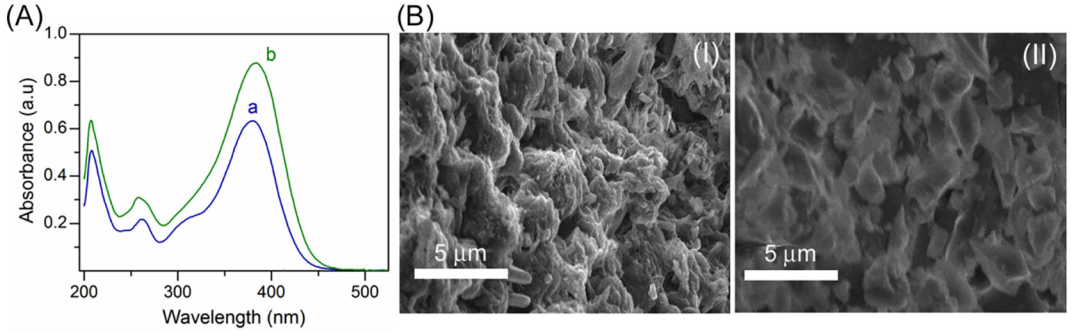

Fig. 2. (A) UV–Vis absorbance spectrum of methanolic solution of (a) butein and (b) butin. (B) SEM images of (I) butein and (II) butin powders.

The FT-IR spectrum of butein reveals the peaks relating to H-bonded OH stretch at 3300 cm^{-1} with distinct shoulder humps at 3478 and 3540 cm^{-1}. The characteristic chalcone group, C=O (conjugated ketone) associated peak is located at 1641 cm^{-1} [38]. The C=C stretching vibrations are observed at 1505, 1552 and 1592 cm^{-1}. Intense peak signals at 1230 and 1348 cm^{-1} are associated to OH in-plane bend. Peaks located at 975 and 1025 cm^{-1} are ascribed to the C–H in-plane bending frequencies. Vibrations of C–H out-of-plane bend were observed in the region 665–855 $cm^{-1.}$ Frequencies located at 540, 586 and 626 cm^{-1} are assigned to the OH out-of-plane bend [39]. The functional group frequencies of butin exhibit significant changes from that of butein. For instance, H-bonded OH stretch is observed at 3310 cm^{-1}. The C=O stretch is moderate at 1636 cm^{-1} and C=C stretching vibrations are observed at 1512 and 1594 cm^{-1}. Signals at 1235, 1284 and 1350 cm^{-1} are attributed to the OH in-plane bending. The characteristic C–O–C stretch of butin is well resolved at 1124 cm^{-1}, supporting the cyclized form of butein structure. C–H in-plane bend signals were at 1030 and 975 cm^{-1}. The C–H out-of-plane bending frequencies were observed in the region 665–850 cm^{-1}. Short but intense peak at 538 and 588 cm^{-1} are attributed to the OH out-of-plane bend [40]. As-observed vibrational signals provide the complementary information on the chemical structure of butein and butin. Structural integrity of butein and butin were also confirmed from ^{1}H NMR spectral analysis which is provided in the supplementary information (Figs. S1 and S2).

Understanding the optical behavior of chemically synthesized phytoconstituents (polyphenols) are highly advantageous for exploring their utility in biomedical imaging. Though the present study is not focused toward bioimaging, the fundamental photoluminescence of the prepared materials was explored to corroborate the chemical structure and its intrinsic emission property. PL spectrum of butein and butin was studied at an excitation wavelength of 378 nm and 382 nm, respectively (Fig. 4A). It can be observed that butein exhibited two well resolved emission peaks in the visible region centered at 486 nm and 522 nm. Similarly butin exhibited two emission bands the first one at 486 nm and the later one at 528 nm, which is slightly red-shifted, compared to butein. Peak intensities of butin emission bands were superior compared to butein. This enhanced emission band is perhaps attributed to the rapid internal conversion of nuclear frameworks *i.e.,* π,π* and n,π* states *via* excited state intramolecular charge transfer (ESICT). Specifically the oxygen group at the 1-position of ring 'C' becomes an electron donor, while the keto oxygen at the 4-position serves as a good electron acceptor, exhibiting effective donor-acceptor conjugation. Although the geometry of butein exhibit ESICT by "keto-enol tautomerization", the steric hindrance due to multiple intermolecular hydrogen bonding with H_2O molecules mediate a weaker fluorescence emission in aqueous environment. Relevant studies on intramolecular proton transfer between hydroxyl and oxygen groups of other flavonoids under mixture of organic-aqueous solvents are available in the literature [6,38,39]. The excited state intramolecular proton transfer was also correlated considering the π electrons in the bonding and anti-

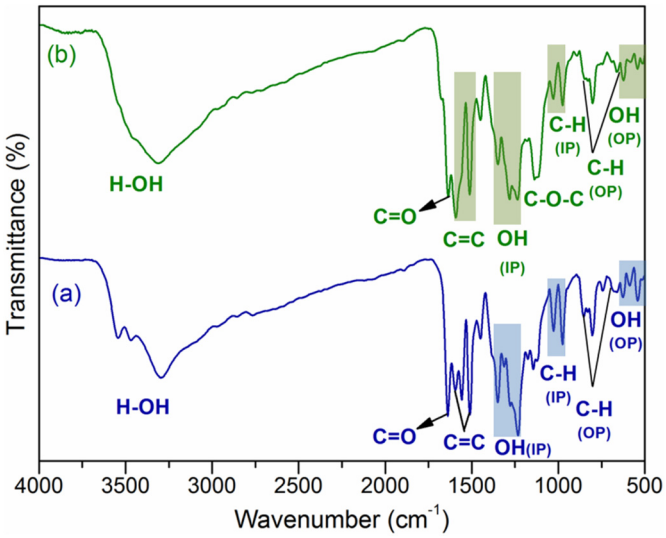

Fig. 3. FT-IR spectrum of (a) butein and (b) butin. IP: in-plane and OP: out-of-plane bends.

bonding characteristic [41].

In order to further understand the stability of photoluminescence of butein and butin a pH dependent study was performed and the results are illustrated in Fig. 4B and C. It can be observed that the emission bands of butein were significantly higher at pH 4 and 5. However, upon increasing the solution pH from 6 to 9, occurrence of intermolecular hydrogen bonding influenced the molecular geometry which hindered the overall ESICT. In the case of butin, existence of three hydroxyl (3′,4′ and 7) and one keto/cyclized oxygen group in ring 'C' have exhibited an altered intermolecular hydrogen bonding characteristics. Such modified nuclear frameworks have expressed an overall intensified emission bands for butin compared to butein. Particularly, at pH 7 aqueous dispersion of butin enabled an amplified emission signal at 486 nm and 528 nm. While at pH 8 and 9, the fluorescence emission peaks are weaker, denoting a steric hindrance. From the above results it can be suggested that the fluorescene emission property of butein and butin can be well resolved at the pH 4–5 and 7, respectively. Presence of combination of keto-enol tautomerization and electron-donor acceptor conjugation has mediated the overall enhancement in the fluorescence emission.

Electrochemical fingerprinting of phytochemicals is useful for qualitative/quantitative validation of herbal formulation. In general, the inherent electrochemical behaviors of flavonoids are depends on the nature of phenoxy radicals generated at the electrode interface [42]. Similar to other organic compounds, the redox properties of flavonoid derivatives are often described by proton-electron transfer with respect to pH, which could also specify the chemico-structural functionality [33]. For instance, flavonoids are weak organic acids and based on the

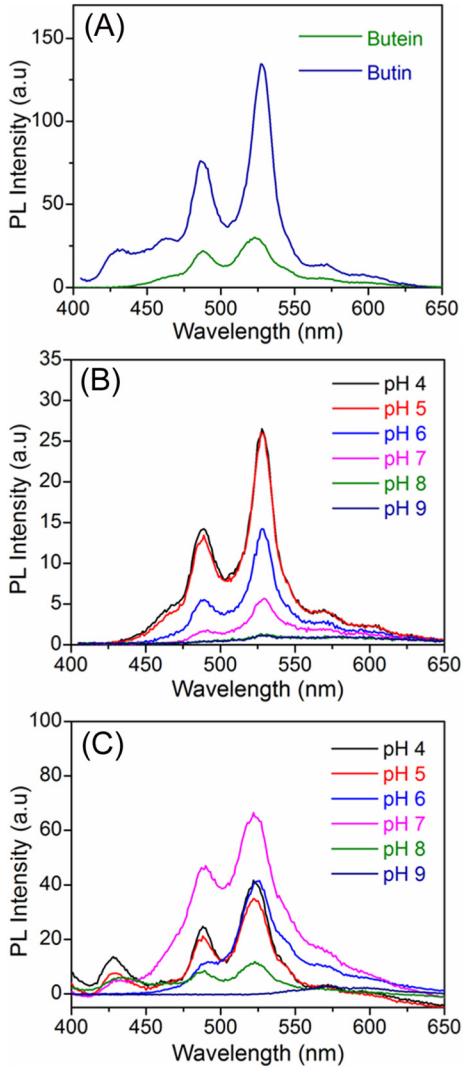

Fig. 4. PL spectra of (A) butein and butin. Effect of solution pH over the PL emission of the (B) butein (at λ_{ex} = 378 nm) and (C) butin (at λ_{ex} = 382 nm).

values of their acid constants, at pH values close to 7 they can be in equilibrium with some of their phenolate ions. It is worth to know that anodic reactions of phenolate ions can be obscured by the existence of dimerization reactions coupled to the initial charge transfer reaction [33,43,44]. In addition to chemical structure of flavonoids and pH of electrolyte solution, electrode material and scan rate may have an interdependent function on the stability of electro-generated radicals during the electrochemical reaction [42,43]. In particular, the structural relationship *i.e.,* the number and position of hydroxyl group substituted in the backbone of flavonoid derivatives play a vital role in the electrochemical behavior [45,46]. Structurally butein have four substituted hydroxyl group in the position 2′,4′ of ring 'A' and 3,4, position of ring 'B', whereas butin have three hydroxyl group substituted at 3′,4′ of ring 'B' and at position 7 of ring 'A' (Fig. 5A).

The cyclic voltammogram (CV) studied for 1.0 mM butein and butin using Au-screen printed electrode in 0.1 M PBS solution of pH 7.2 at a scan rate of 0.1 Vs^{-1} is illustrated in Fig. 5B. The first anodic peak potential (E_{pa1}) appeared at +0.73 V with a low current intensity is attributed to the resorcinol type OH group (2′ and 4′) in the 'A' ring of butein [42,46,47]. Anodic peaks at +0.93 V (E_{pa2}) and +1.4 V (E_{pa3}) are ascribed to the oxidation of catechol type OH group at the position 3 and 4 in the 'B' ring of butein. The characteristic single broad cathodic peak potential (E_{pc1}) centered at +0.37 V is corresponding to the reduction of quinone species. Unlike butein, CV study of butin exhibit a single anodic peak potential which is moderately broader than E_{pa2} of butein, centered at +0.94 V. The reduction peak potential for butin is observed at less positive potential +0.25 V. Mechanism behind this redox peak potential could be related to the specific solvation effect on the hydroxyl moieties. Earlier studies have reported that phenolic groups in B-ring undergo oxidation reaction at lower potential compared to the OH-group of A-ring [45,47]. The reversibility is also relevant to the electron delocalization magnitude in *para* and *ortho* positions, which could mediate the stabilization of phenoxy radicals and minimizes the necessity of overpotential [46,47]. Similar to isoflavones, butin structure is slightly acidic compared to butein owing to the existence of three hydroxyl group. It is assumed that the intermediates generated from phenoxy radicals at A and B ring reduces at lower potential owing to the fact of inherent electron/proton donor ability. Fig. 5C and E represents the CVs of butein and butin at different scan rates (0.01–0.1 Vs^{-1}). The significant enhancement in the oxidation/reduction reaction peak current was in relation to the scan rate (Fig. 5D and F) and the linear relationship for CVs of butein was found to be 0.97 (I_{pa}) and 0.98 (I_{pc}) and butin was found to be 0.99 (I_{pa}) and 0.99 (I_{pc}). Fig. 5D anodic peak current linearity trace is attributed from the I_{pa2} at +0.93 V of Fig. 5C.

Fig. 6A represents the CVs of 1 mM butein in PBS at different pH. As can be seen the E_{pa1} at +0.73 V is weakly expressive at pH 4–6, while at pH 7–9 the peak current is moderately increased. Particularly, the overall anodic peak current intensity of butein at pH 8 is superior compared to pH 7 and 9. It is also worth mentioning that with increase of pH the inherent E_{pa2} and E_{pa3} at +0.93 V and +1.4 V (ascribed to the quinone species) are continuously shifting toward the higher positive potential region. This transition perhaps related to the deprotonation and protonation of the phenoxy radicals exist at the 'B' ring of butein.

Transformation of oxidized quinone moieties into semiquinone and hydroquinone, upon sequential reduction reaction is observed to be pH dependent [48,49]. Fig. 6B illustrates the pH dependent CV behavior of butin samples. It can be observed that alteration of electrolyte's pH from 4 to 9 have no significant influence on the anodic peak potential of butin except minimal changes in the peak current intensity. Whereas, the cathodic peak potential have noticeable shift in the positive region with respect to increase of pH. For instance, at pH 4 E_{pc} of butin was at +0.17 V, while at pH 5 and 6 it is shifted to +0.24 V and +0.22 V, respectively. From pH 7–9 there were no major changes in the cathodic peak potential (+0.26 V) and current. This observation perhaps related to the structural integrity of electroactive hydroxyl group position in the butin moiety. The molecular behavior relevant to protonation and deprotonation of phenoxy radicals located at position 7 of ring 'A', position 3′ and 4′ of ring 'B' is governed by interfacial phenomena. Reports have discussed that molecular orientation of quinone redox species, from other polyphenol, and its specific interaction at electrode interface are dependent on various interfacial phenomena such as polarity of the solvents, intra or intermolecular hydrogen bonding of neighboring group, presence of acidic or basic additives and ion pairing [50].

In order to explore the direct electrochemical detection feasibility of pure butein and butin, herein, a fundamental CV study on different concentrations were tested using Au-screen printed electrode (SPE) as the working interface in the optimal potential region +0.0 V to +1.5 V. As shown in Fig. 7A, the anodic peak current increases with increasing concentration of butein. Similarly, butin redox behavior is also significantly distinguishable with increase of concentrations (Fig. 7B), indicating the direct electron-transfer at the electrode interface. Observed experimental results suggest that the bare Au-SPE is capable of discriminating the inherent structural integrity of butein and butin. Mainly, the existence of electroactive hydroxyl groups makes this group

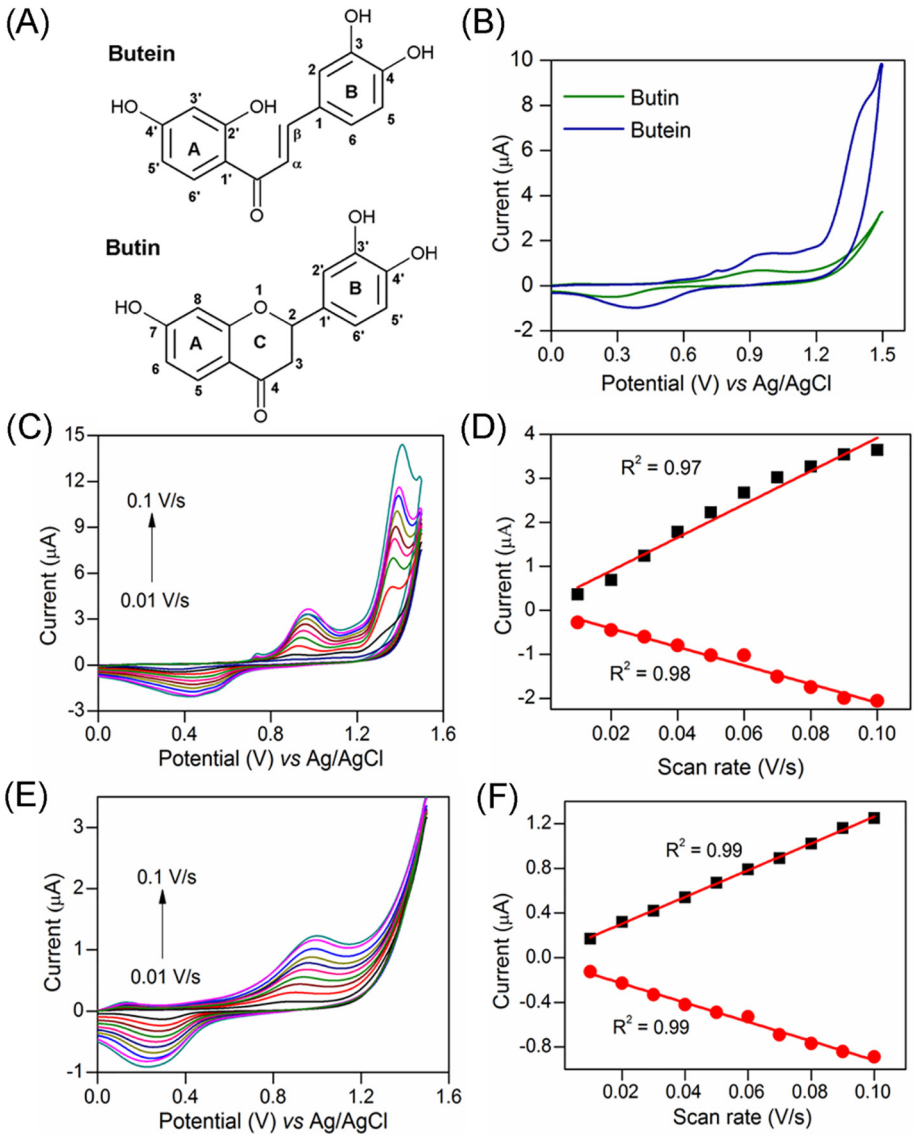

Fig. 5. (A) Chemical structure of butein and butin. (B) Cyclic voltammogram of butein (1 mM) and butin (1 mM) in 0.1 M PBS buffer (pH 7.2), scan rate 0.1 Vs^{-1}. (C) Cyclic voltammograms of (C) butein and (E) butin at different scan rates (0.01–0.1 Vs^{-1}) and (D and F) the corresponding plots of peak currents against scan rates.

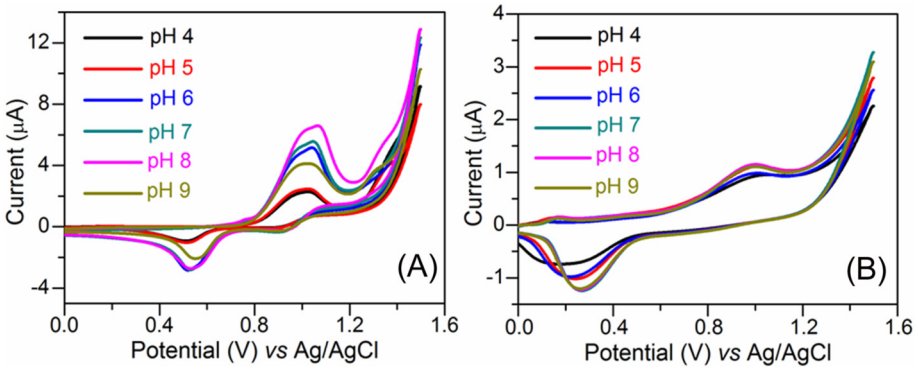

Fig. 6. CVs of (A) butein and (B) butin measured at Au-screen printed electrode (Au-SPE) in 0.1 M PBS with respect to various pH conditions.

of flavonoids unique and fingerprinting them using modern electrode materials could extend their real-time application in phytochemical industries. Further, demonstration on optical (UV–vis absorbance and PL emission) and electrochemical functionality of this clinically important polyphenols not only provides their structural property but also exposed the new materials function similar to inorganic/organic plasmonic nanostructures. Perhaps the observed inherent photoluminescence and redox behavior of butein/butin are potential for exploration toward *in situ* bioimaging and biosensor.

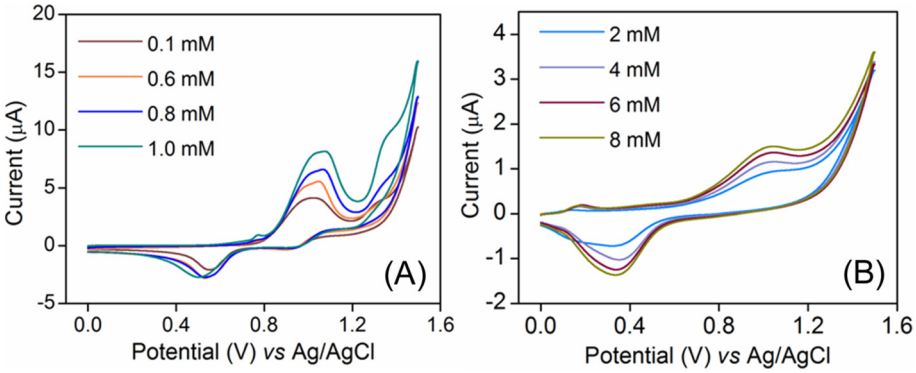

Fig. 7. Concentration dependent voltammetric behavior of (A) butein and (B) butin at Au-SPE in 0.1 M PBS (pH 7.2), scan rate 0.1 V s^{-1}.

4. Conclusion

Chalcone and flavanone types of polyphenols are chemically synthesized. UV–vis absorbance studies demonstrated the distinct $\pi \rightarrow \pi^*$ and $n \rightarrow \pi^*$ transition bands of butein and butin. FT-IR and ^{1}H NMR results evidenced the structural integrity of butein and butin related to chalcone type C=O and flavanone type C-O-C stretch. Topography of butein and butin powder samples visualized from SEM supports that the chemically synthesized polyphenols resembles crystal-like structure. PL spectral analysis revealed that both butein and butin exhibit well resolved visible light (blue and green) emission bands in aqueous environment. pH dependent PL studies enabled that butein and butin samples exhibit better emission signals at pH 4–5 and 7, respectively. Primitive cyclic voltammetric investigations on butein/butin samples at Au-SPE interface suggest that their redox behavior are distinct governed by the location of electroactive OH groups at ring 'A' and 'B'. Transition of phenoxy radicals of butein/butin generated during the redox reactions evaluated under various pH are useful for sensor studies. Fundamental direct electron-transfer reaction of butein/butin demonstrated at the interface of Au-SPE may find potentiality for cost-efficient and rapid validation of polyherbal formulation constituting chalcone/flavanone.

Acknowledgments

Authors acknowledge the Department of Pharmaceuticals, Ministry of Chemicals and Fertilizers, Government of India for their financial assistance. M. Veerapandian acknowledges the CSIR-Central Electrochemical Research Institute, Karaikudi, for providing the start-up grant (IHP-0112).

Appendix A. Supplementary Data

Supplementary data to this article can be found online at https://doi.org/10.1016/j.jphotobiol.2018.04.001.

References

[1] M. Veerapandian, P.K. Avti, V. Ravichandiran, Ruthenium bipyridine sensitized MoO_3 multifunctional nanostructures: study of opto-electrochemical properties, biocompatibility and bioimaging, Colloid Surf. B 154 (2017) 315–320.
[2] M. Veerapandian, N. Lévaray, M.H. Lee, S. Giasson, X.X. Zhu, Glucosamine-anchored graphene oxide nanosheets: fabrication, ultraviolet irradiation, and electrochemical properties, ACS Appl. Mater. Interfaces 7 (2015) 14552–14556.
[3] R.B. Semwal, D.K. Semwal, S. Combrinck, A. Viljoen, Butein: from ancient traditional remedy to modern nutraceutical, Phytochem. Lett. 11 (2015) 188–201.
[4] J.B. Harborne, C.A. Williams, Advances in flavonoid research since 1992, Phytochemistry 55 (2000) 481–504.
[5] N.E. Es-Safi, S. Ghidouche, P.H. Ducrot, Flavonoids: hemisynthesis, reactivity, characterization and free radical scavenging activity, Molecules 12 (2007) 2228–2258.
[6] H.R. Park, Y. Daun, J.K. Park, K.M. Bark, Spectroscopic properties of flavonids in various aqueous-organic solvent mixtures, Bull. Kor. Chem. Soc. 34 (2013) 211–220.
[7] A. Mbonyiryivuze, I. Omollo, B.D. Ngom, B. Mwakikunga, S.M. Dhlamini, E. Park, M. Maaza, Natural dye sensitizer for Grätzel cells: sepia melanin, Phys. Mater. Chem. 3 (2015) 1–6.
[8] A. Mbonyiryivuze, Z.Y. Nuru, B.D. Ngom, B. Mwakikunga, S.M. Dhlamini, E. Park, M. Maaza, Morphological and chemical composition characterization of commercial Sepia melanin, Am. J. Nanomater. 3 (2015) 22–27.
[9] M. Khenfouch, O. Bajjou, M. Baïtoul, N. Mongwaketsi, M. Maaza, J. Wery Venturini, Optical properties and dynamics excitation relaxation in reduced graphene oxide functionalized with nanostructured porphyrins, Opt. Mater. 42 (2015) 479–483.
[10] N. Mongwaketsi, L. Kotsedi, Z. Nuru, R. Sparrow, G. Garab, M. Maaza, Porphyrin nanorods-polymer composites for solar radiation harvesting applications, J. Porphyrins Phthalocyanines 18 (2014) 1145–1156.
[11] N. Mongwaketsi, S. Khamlich, M. Pranaitis, B. Sahraoui, F. Khammar, G. Garab, R. Sparrow, M. Maaza, Physical origin of third order non-linear optical response of porphyrin nanorods, Mater. Chem. Phys. 134 (2012) 646–650.
[12] S. Kumar, A.K. Pandey, Chemistry and biological activities of flavonoids: an overview, Sci. World J. 162750 (2013) 1–16.
[13] E.B. Yang, K. Zhang, L.Y. Cheng, P. Mack, Butein, a specific protein tyrosine kinase inhibitor, Biochem. Biophys. Res. Commun. 245 (1998) 435–438.
[14] Y.N. Chen, T.F. Huang, C.H. Chang, C.C. Hsu, K.T. Lin, S.W. Wang, H.C. Peng, C.H. Chung, Antirestenosis effect of butein in the neointima formation progression, J. Agric. Food Chem. 60 (2012) 6832–6838.
[15] N.Y. Kim, H.O. Pae, G.S. Oh, T.H. Kang, Y.C. Kim, H.Y. Rhew, H.T. Chung, Butein, a plant polyphenol, induces apoptosis concomitant with increased caspase-3 activity, decreased Bcl-2 expression and increased Bax expression in HL-60 cells, Pharmacol. Toxicol. 88 (5) (2001) 261–266.
[16] Y. Wang, F.L. Chan, S. Chen, L.K. Leung, The plant polyphenol butein inhibits testosterone-induced proliferation in breast cancer cells expressing aromatase, Life Sci. 77 (1) (2005) 39–51.
[17] C.C. Yit, N.P. Das, Cytotoxic effect of butein on human colon adenocarcinoma cell proliferation, Cancer Lett. 82 (1) (1994) 65–72.
[18] S.H. Lee, G.S. Seo, H.S. Kim, S.W. Woo, G. Ko, D.H. Sohn, 2′,4′,6′- Tris(methoxymethoxy) chalcone attenuates hepatic stellate cell proliferation by a heme oxygenase-dependent pathway, Biochem. Pharmacol. 72 (10) (2006) 1322–1333.
[19] M.H. Park, I.S. Kim, S.A. Kim, C.S. Na, C.Y. Hong, M.S. Dong, H.H. Yoo, Inhibitory effect of Rhusverniciflua Stokes extract on human aromatase activity; butin is its major bioactive component, Bioorg. Med. Chem. Lett. 24 (7) (2014) 1730–1733.
[20] G. Aldini, L. Regazzoni, A. Pedretti, M. Carini, S.M. Cho, K.M. Park, K.J. Yeum, An integrated high resolution mass spectrometric and informatics approach for the rapid identification of phenolics in plant extract, J. Chromatogr. A 1218 (2011) 2856–2864.
[21] M. Veerapandian, R. Subbiah, G.-S. Lim, S.H. Park, K.S. Yun, M.H. Lee, Copper-glucosamine microcubes: synthesis, characterization, and C-reactive protein detection, Langmuir 27 (2011) 8934–8942.
[22] M. Veerapandian, Y.T. Seo, K.S. Yun, M.H. Lee, Graphene oxide functionalized with silver@silica–polyethylene glycol hybrid nanoparticles for direct electrochemical detection of quercetin, Biosens. Bioelectron. 58 (2014) 200–204.
[23] J.A. Ribeiro, C.M. Pereira, A.F. Silva, M.G.F. Sales, Electrochemical detection of cardiac biomarker myoglobin using polyphenol as imprinted polymer receptor, Anal. Chim. Acta 981 (2017) 41–52.
[24] M. Sengan, D. Veeramuthu, A. Veerappan, Photosynthesis of silver nanoparticles using *Durio zibethinus* aqueous extract and its application in catalytic reduction of nitroaromatics, degradation of hazardous dyes and selective colorimetric sensing of mercury ions, Mater. Res. Bull. 100 (2018) 386–398.
[25] F.Lima.B.G. Lucca, A.M.J. Barbosa, V.S. Ferreira, S.K. Moccelini, A.C. Franzoi, I.C. Vieira, Biosensor based on pequi polyphenol oxidase immobilized on chitosan crosslinked with cyanuric chloride for thiodicarb determination, Enzym. Microb. Technol. 47 (2010) 153–158.
[26] C. Topcu, B. Caglar, A. Onder, F. Coldur, S. Caglar, E.K. Guner, O. Cubuk, A. Tabak, Structural characterization of chitosan-smectite nanocomposite and its application in the development of a novel potentiometric monohydrogen phosphate-selective sensor, Mater. Res. Bull. 98 (2018) 288–299.
[27] B. Gómez-Zaleta, M.T. Ramírez-Silva, A. Gutiérrez, E. González-Vergara, M. Güizado-Rodríguez, A. Rojas-Hernández, UV/vis, ^{1}H, and ^{13}C NMR

spectroscopic studies to determine mangiferin pKa values, Spectrochim. Acta A 64 (2006) 1002–1009.
[28] S. Tajik, M. Taher, H. Beitollahi, The first electrochemical sensor for determination of mangiferin based on an ionic liquid–graphene nanosheets paste electrode, Ionics 20 (2014) 1155–1161.
[29] M.J. Sims, Q. Li, R.T. Kachoosangi, G.G. Wildgoose, R.G. Compton, Using multi-walled carbon nanotube modified electrodes for the adsorptive striping voltammetric determination of hesperidin, Electrochim. Acta 54 (2009) 5030–5034.
[30] L. Wang, Q. Wang, K. Sheng, G. Li, B. Ye, A new graphene nanocomposite modified electrode as efficient voltammetric sensor for determination of eriocitrin, J. Electroanal. Chem. 785 (2017) 96–102.
[31] Z. Xie, W. Lu, L. Yang, G. Li, B. Ye, A voltammetry sensor platform for baicalein and baicalin simultaneous detection in vivo based on Ta_2O_5-Nb_2O_5@CTS composite, Talanta 170 (2017) 358–368.
[32] W.F. Hodnick, E.B. Milosavljevic, J.H. Nelson, R.S. Pardini, Electrochemistry of flavonoids. Relationships between redox potentials, inhibition of mitochondrial respiration, and production of oxygen radical by flavonoids, Biochem. Pharmacol. 37 (1988) 2607–2611.
[33] A.Y. Tesio, S.N. Robledo, H. Fernández, M.A. Zon, Electrochemical oxidation of butein at glassy carbon electrodes, Bioelectrochemistry 91 (2013) 62–69.
[34] G.M. Sanchez, J.P. Rosazza, Biocatalytic synthesis of butein and sulfuretin by *Aspergillus alliaceus*, J. Agric. Food Chem. 54 (2006) 4646–4650.
[35] S. Ohno, M. Hosokawa, A. Hoshino, Y. Kitamura, Y. Morita, K.I. Park, A. Nakashima, A. Deguchi, F. Tatsuzawa, M. Doi, S. Iida, S. Yazawa, A bHLH transcription factor, DvIVS, is involved in regulation of anthocyanin synthesis in dahlia (Dahlia variabilis), J. Exp. Bot. 62 (2011) 5105–5116.
[36] Y.H. Seo, Butein disrupts Hsp90′s molecular chaperoning function and exhibits anti-proliferative effects against drug-resistant Cancer cells, Bull. Kor. Chem. Soc. 34 (2013) 3345–3349.
[37] S.V. Vuppalapati, L. Xia, N. Edayadulla, Y.R. Lee, Mild and efficient one-pot synthesis of diverse flavanone derivatives via an organocatalyzed mannich-type reaction, Synthesis 46 (2014) 465–474.
[38] M.R. Rajalakshmy, G. Geetha, Isolation and identification of withasomnine, withanolides and butein from industrial herbal marc of *Withania somnifera* (L.) Dunal, Indian J. Nat. Prod. Resour. 7 (2016) 116–124.
[39] J. Coates, Interpretation of infrared spectra, a practical approach, in: R.A. Meyers (Ed.), Encyclopedia of Analytical Chemistry, John Wiley and Sons Ltd., Chichester, UK, 2000, pp. 10815–10837.
[40] N. Matías Funes, M. Correa, J.J. Silber, M.A. Biasutti, Comparative study of the photophysical behavior of fisetin in homogeneous media and in anionic and cationic reverse micelles media, Photochem. Photobiol. 83 (2007) 486–493.
[41] H.R. Park, H.B. Liu, S.C. Shin, J.K. Park, K.M. Bark, Spectroscopic properties of Quercetin-3-O-rhamnoside and Quercetin-3-O-rutinoside in aerosol-OT reverse micelles, Bull. Kor. Chem. Soc. 32 (2011) 981–998.
[42] T.A. Enache, A.M. Oliveira-Brett, Phenol and parasubstituted phenols electrochemical oxidation pathways, J. Electroanal. Chem. 655 (2011) 9–16.
[43] I.E. Mülazımoğlu, E. Özkan, A.O. Solak, High energetic body source and strong antioxidant quercetin, morin and rutin: their covalent grafting onto the glassy carbon electrode surfaces and investigation of surface properties, Energy Educ. Sci. Tech. A 28 (2012) 957–968.
[44] S. Martinez, L. Valek, Z. Petrovic, M. Metikos-Hukovic, J. Piljac, Catechin antioxidation action at various pH studied by cyclic voltammetry and PM3 semi-empirical calculations, J. Electroanal. Chem. 584 (2005) 92–99.
[45] E.S. Gil, R.O. Couto, Flavonoid electrochemistry: a review on the electroanalytical applications, Braz. J. Pharmacogn. 23 (2013) 542–558.
[46] B. Nasr, G. Abdellatif, P. Cañizares, C. Sáez, J. Lobato, M.A. Rodrigo, Electrochemical oxidation of hydroquinone, resorcinol, and catechol on boron-doped diamond anodes, Environ. Sci. Technol. 39 (2005) 7234–7239.
[47] D. Zhang, L. Chu, Y. Liu, A. Wang, B. Ji, W. Wu, F. Zhou, Y. Wei, Q. Cheng, S. Cai, L. Xie, G. Jia, Analysis of the antioxidant activity capacities of flavonoids under different spectrophotometric assays using cyclic voltammetry and density functional theory, J. Agrc. Food Chem. 59 (2011) 10277–10285.
[48] A. Okamoto, K. Hashimoto, K.H. Nealson, R. Nakamura, Rate enhancement of bacterial extracellular electron transport involves bound flavin semiquinones, Proc. Natl. Acad. Sci. U.S. A. 110 (2013) 7856.
[49] Y. Wu, F. Li, T. Liu, R. Han, X. Luo, pH dependence of quinone-mediated extracellular electron transfer in a bioelectrochemical system, Electrochim. Acta 213 (2016) 408–415.
[50] P. Guin, S. Das, P.C. Mandal, Electrochemical reduction of quinones in different media: a review, Int. J. Electrochem. 816202 (2011) (22 pages).